

HADRON PROPERTIES IN NUCLEAR MEDIUM AND THEIR IMPACTS ON OBSERVABLES

K. TSUSHIMA

*Department of Physics and Astronomy, University of Georgia
Athens, GA 30602, USA
E-mail: tsushima@physast.uga.edu*

The effect of changes in hadron properties in a nuclear medium on physical observables is discussed. Highlighted results are, (1) hypernuclei, (2) meson-nuclear bound states, (3) K -meson production in heavy ion collisions, and (4) J/Ψ dissociation in a nuclear medium. In addition, results for the near-threshold ω - and ϕ -meson production in proton proton collisions are reported.

1. Hadrons in nuclear medium: treatment in QMC ^{1,2,3,4,5,6,7,8}

We discuss here hadrons in a nuclear medium in quark-meson coupling (QMC) model ¹. The model has been extended and successfully applied to many problems ^{2,3,4,5,6,7,8}. A detailed description of the Lagrangian density, the mean-field equations of motion, and the treatment of finite nuclei are given in Refs. ^{2,3}. As examples, we show in Fig. 1 results for ^{40}Ca nucleus in QMC ³, which bases on the quark structure of nucleon, or, nucleus.

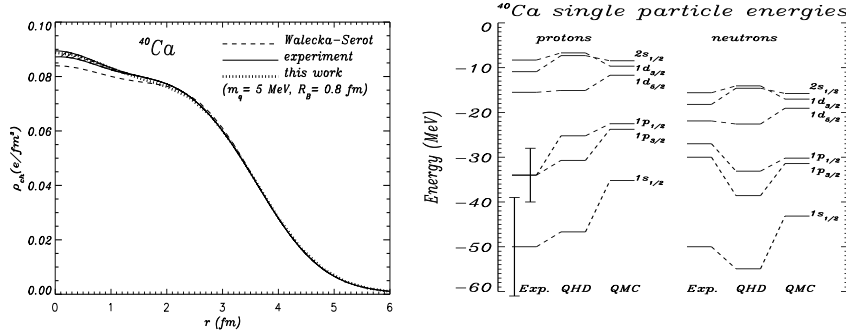


Figure 1. Charge density distribution (the left panel) and energy spectrum (the right panel) for ^{40}Ca nucleus, compared with the experimental data and those of Quantum Hadrodynamics (QHD, also labeled by “Walecka-Serot”) ¹⁰.

The Dirac equations for the quarks and antiquarks in hadron bags ($q = u, \bar{u}, d$ or \bar{d} , hereafter) neglecting the Coulomb force, are given by ($|\mathbf{x}| \leq$ bag radius) ^{2,3,4,5,6,7,8}:

$$\left[i\boldsymbol{\gamma} \cdot \partial_x - (m_q - V_\sigma^q) \mp \gamma^0 \left(V_\omega^q + \frac{1}{2} V_\rho^q \right) \right] \begin{pmatrix} \psi_u(x) \\ \psi_{\bar{u}}(x) \end{pmatrix} = 0, \quad (1)$$

$$\left[i\gamma \cdot \partial_x - (m_q - V_\sigma^q) \mp \gamma^0 \left(V_\omega^q - \frac{1}{2} V_\rho^q \right) \right] \begin{pmatrix} \psi_d(x) \\ \psi_{\bar{d}}(x) \end{pmatrix} = 0, \quad (2)$$

$$[i\gamma \cdot \partial_x - m_{s,c}] \psi_{s,c}(x) \text{ (or } \psi_{\bar{s},\bar{c}}(x)) = 0. \quad (3)$$

The mean-field potentials for a bag in nuclear matter are defined by $V_\sigma^q \equiv g_\sigma^q \sigma$, $V_\omega^q \equiv g_\omega^q \omega$ and $V_\rho^q \equiv g_\rho^q b$, with g_σ^q , g_ω^q and g_ρ^q the corresponding quark-meson coupling constants. The bag radius in medium for a hadron h , R_h^* , will be determined through the stability condition for the mass of the hadron against the variation of the bag radius^{1,2} (see Eq. (4)). The hadron masses in a nuclear medium m_h^* (free mass will be denoted by m_h), are calculated by

$$m_h^* = \sum_{j=q,\bar{q},Q,\bar{Q}} \frac{n_j \Omega_j^* - z_h}{R_h^*} + \frac{4}{3} \pi R_h^{*3} B, \quad \left. \frac{\partial m_h^*}{\partial R_h} \right|_{R_h=R_h^*} = 0, \quad (4)$$

where $\Omega_q^* = \Omega_{\bar{q}}^* = [x_q^2 + (R_h^* m_q^*)^2]^{1/2}$ ($q = u, d$), with $m_q^* = m_q - g_\sigma^q \sigma$, $\Omega_Q^* = \Omega_{\bar{Q}}^* = [x_Q^2 + (R_h^* m_Q)^2]^{1/2}$ ($Q = s, c$), and $x_{q,Q}$ being the bag eigenfrequencies. B is the bag constant, $n_q(n_{\bar{q}})$ and $n_Q(n_{\bar{Q}})$ are the lowest mode quark (antiquark) numbers for the quark flavors q and Q in the hadron h , respectively, and the z_h parametrize the sum of the center-of-mass and gluon fluctuation effects (assumed to be independent of density). The parameters are determined in free space to reproduce the corresponding masses. We chose the values, $(m_q, m_s, m_c) = (5, 250, 1300)$ MeV for the current quark masses, and $R_N = 0.8$ fm for the bag radius of the nucleon in free space. The quark-meson coupling constants, g_σ^q , g_ω^q and g_ρ^q , are adjusted to fit the nuclear saturation energy and density of symmetric nuclear matter, and the bulk symmetry energy². However, in studies of the kaon system, we found that it was phenomenologically necessary to increase the strength of the vector coupling to the non-strange quarks in the K^+ (by a factor of 1.4², i.e., $g_{K\omega}^q \equiv 1.4^2 g_\omega^q$) in order to reproduce the empirically extracted K^+ -nucleus interaction⁵. We assume this also for the D and \bar{D} mesons^{7,8,9}. The scalar (V_s^h) and vector (V_v^h) potentials felt by the hadrons h , in nuclear matter are given by,

$$V_s^h = m_h^* - m_h, \quad V_v^h = (n_q - n_{\bar{q}}) V_\omega^q - I_3 V_\rho^q \quad (V_\omega^q \rightarrow 1.4^2 V_\omega^q \text{ for } K, \bar{K}, D, \bar{D}), \quad (5)$$

where I_3 is the third component of isospin projection of the hadron h .

In Fig. 2 we show effective masses and mean field potentials for various hadrons in symmetric nuclear matter. Several comments are on the results shown in Fig. 2:

- (1) Physical η and η' mesons are treated including mixing angle, $\theta_P = -10^\circ$, as $(\eta, \eta') = (\eta_8 \cos \theta_P - \eta_1 \sin \theta_P, \eta_8 \sin \theta_P + \eta_1 \cos \theta_P)$, where $\eta_1 = (1/\sqrt{3})(u\bar{u} + d\bar{d} + s\bar{s})$ and $\eta_8 = (1/\sqrt{6})(u\bar{u} + d\bar{d} - 2s\bar{s})$.

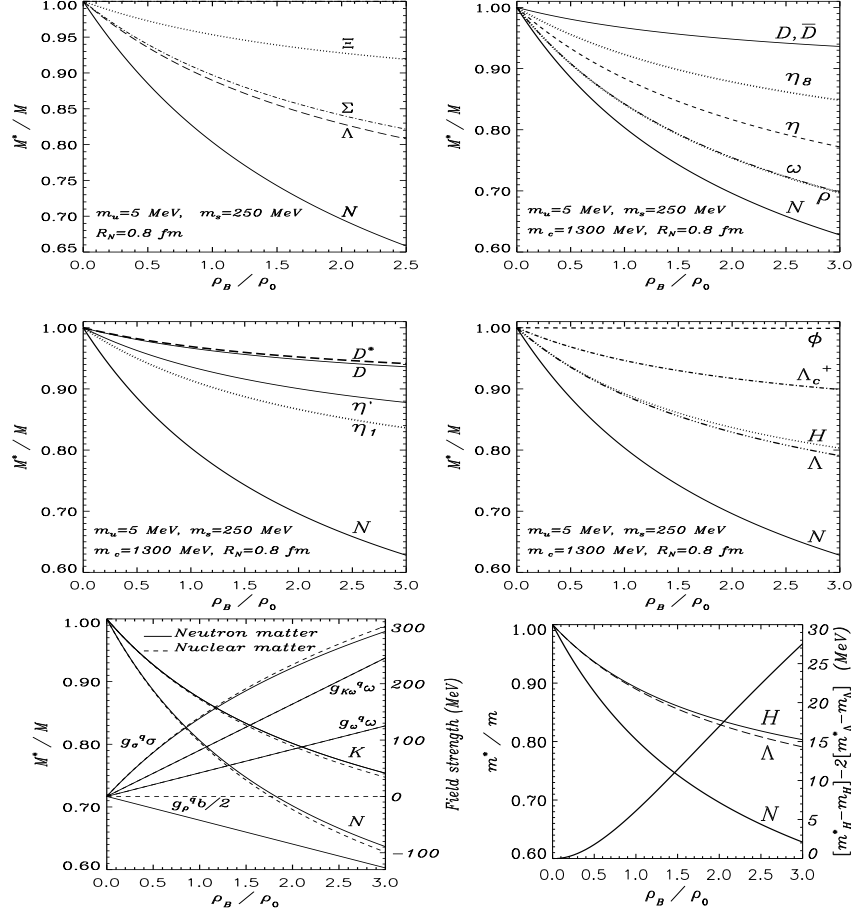


Figure 2. Effective mass ratios and mean field potentials for hadrons in nuclear matter ($\rho_0 = 0.15 \text{ fm}^{-3}$). “H” stands for the H particle with an input $m_H = 2m_\Lambda$.

- (2) The H particle is treated as a 6-quark bag, $uuddss$, with $m_H = 2m_\Lambda$.
- (3) The scalar potential for the hadron h , V_s^h , shows a universal quark number scaling rule, $V_s^h/V_s^N \simeq (n_q + n_{\bar{q}})/3$, where V_s^N is the scalar potential for the nucleon. (See Eq. (5).)
- (4) The scalar potential for the ϕ meson arises entirely from the $\phi - \omega$ mixing in QMC, and tiny.
- (5) Reduction in effective mass for the Λ_c^+ implies the role of the light quarks in partial restoration of chiral symmetry in a heavy-light quark system, and has a merit of further study.

In following sections we will discuss how these changes in hadron properties in a nuclear medium give impacts on physical observables.

2. Hypernuclei ⁴

When a hyperon, Y , is embedded in a nucleus, the potential felt by the hyperon at a given position of the nucleus can be calculated self-consistently ⁴. Simultaneously one can get also energy levels for the hyperon Y in a shell-model calculation ⁴. Because the treatment is based on the quark degrees of freedom, we need to consider a possibility of Pauli blocking effect at the quark level, and also effect of Σ - Λ channel coupling for the Σ - and Λ -hypernuclei. We included these effects in a phenomenological way ⁴. Nevertheless, we can study all Λ -, Σ -, Ξ -hypernuclei in a systematic way, due to the quark degrees of freedom, because the hyperon-meson coupling constants in nuclear medium are automatically determined ⁴. In Table 1 we present QMC predictions for the energy levels of hyperons in various hypernuclei. Results for other heavier mass hypernuclei are given in Ref. ⁴.

Table 1. Energy levels for hyperons Y (in MeV), for ^{17}O , ^{41}Ca and ^{49}Ca hypernuclei, calculated in QMC. Experimental data are taken from Ref. ¹¹.

	$^{16}\Lambda\text{O}$ (Expt.)	$^{17}\Lambda\text{O}$	$^{17}\Sigma^-\text{O}$	$^{17}\Sigma^0\text{O}$	$^{17}\Sigma^+\text{O}$	$^{17}\Xi^-\text{O}$	$^{17}\Xi^0\text{O}$
$1s_{1/2}$	-12.5	-14.1	-17.2	-9.6	-3.3	-9.9	-4.5
$1p_{3/2}$		-5.1	-8.7	-3.2	—	-3.4	—
$1p_{1/2}$	-2.5 (1p)	-5.0	-8.0	-2.6	—	-3.4	—
	$^{40}\Lambda\text{Ca}$ (Expt.)	$^{41}\Lambda\text{Ca}$	$^{41}\Sigma^-\text{Ca}$	$^{41}\Sigma^0\text{Ca}$	$^{41}\Sigma^+\text{Ca}$	$^{41}\Xi^-\text{Ca}$	$^{41}\Xi^0\text{Ca}$
$1s_{1/2}$	-20.0	-19.5	-23.5	-13.4	-4.1	-17.0	-8.1
$1p_{3/2}$		-12.3	-17.1	-8.3	—	-11.2	-3.3
$1p_{1/2}$	-12.0 (1p)	-12.3	-16.5	-7.7	—	-11.3	-3.4
$1d_{5/2}$		-4.7	-10.6	-2.6	—	-5.5	—
$2s_{1/2}$		-3.5	-9.3	-1.2	—	-5.4	—
$1d_{3/2}$		-4.6	-9.7	-1.9	—	-5.6	—
	—	$^{49}\Lambda\text{Ca}$	$^{49}\Sigma^-\text{Ca}$	$^{49}\Sigma^0\text{Ca}$	$^{49}\Sigma^+\text{Ca}$	$^{49}\Xi^-\text{Ca}$	$^{49}\Xi^0\text{Ca}$
$1s_{1/2}$		-21.0	-19.3	-14.6	-11.5	-14.7	-12.0
$1p_{3/2}$		-13.9	-11.4	-9.4	-7.5	-8.7	-7.4
$1p_{1/2}$		-13.8	-10.9	-8.9	-7.0	-8.8	-7.4
$1d_{5/2}$		-6.5	-5.8	-3.8	-2.0	-3.8	-2.1
$2s_{1/2}$		-5.4	-6.7	-2.6	—	-4.6	-1.1
$1d_{3/2}$		-6.4	-5.2	-3.1	-1.2	-3.8	-2.2
$1f_{7/2}$		—	-1.2	—	—	—	—

3. Meson-nuclear bound states ^{6,7}

Next, we discuss the meson-nuclear bound states. We have solved the Klein-Gordon equation for mesons j ($j = \omega, \eta, \eta', D, \bar{D}$) with the situation of almost zero momenta, using the calculated potentials in QMC ^{6,7}:

$$[\nabla^2 + E_j^{*2} - \tilde{m}_j^{*2}(r)] \phi_j(\vec{r}) = 0, \quad E_j^* \equiv E_j + m_j - i\Gamma_j/2, \quad (6)$$

$$\tilde{m}_j^*(r) \equiv m_j^*(r) - \frac{i}{2} [(m_j - m_j^*(r))\gamma_j + \Gamma_j] \equiv m_j^*(r) - \frac{i}{2}\Gamma_j^*(r), \quad (7)$$

where E_j^* is the complex valued, total energy of the meson, and we included the widths of the mesons in a nucleus assuming a specific form using γ_j , which are treated as phenomenological parameters. We calculate the single-particle energies for the values $\gamma_\omega = 0.2$, and $\gamma_\eta = 0.5$, which are expected to correspond best with experiments ⁶, while for the η' , D and \bar{D} , the widths $\Gamma_j^* = 0$ are assumed ⁷. For a comparison we present also results for the ω calculated using the potentials obtained in QHD ¹². Results are given in Tables 2 and 3.

Table 2. Calculated ω -, η - and η' -nuclear bound state energies (in MeV), $E_j = \text{Re}(E_j^* - m_j)$ ($j = \omega, \eta, \eta'$), in QMC ⁶ and those for the ω in QHD with σ - ω mixing effect ¹². The complex eigenenergies are given by, $E_j^* = E_j + m_j - i\Gamma_j/2$. (* not calculated)

		$\gamma_\eta = 0.5$	(QMC)	(QMC)	$\gamma_\omega = 0.2$	(QMC)	$\gamma_\omega = 0.2$	(QHD)
		E_η	Γ_η	$E_{\eta'}$	E_ω	Γ_ω	E_ω	Γ_ω
⁶ He	1s	-10.7	14.5	*	-55.6	24.7	-97.4	33.5
¹¹ B	1s	-24.5	22.8	*	-80.8	28.8	-129	38.5
²⁶ Mg	1s	-38.8	28.5	*	-99.7	31.1	-144	39.8
	1p	-17.8	23.1	*	-78.5	29.4	-121	37.8
	2s	—	—	*	-42.8	24.8	-80.7	33.2
¹⁶ O	1s	-32.6	26.7	-41.3	-93.4	30.6	-134	38.7
	1p	-7.72	18.3	-22.8	-64.7	27.8	-103	35.5
⁴⁰ Ca	1s	-46.0	31.7	-51.8	-111	33.1	-148	40.1
	1p	-26.8	26.8	-38.5	-90.8	31.0	-129	38.3
	2s	-4.61	17.7	-21.9	-65.5	28.9	-99.8	35.6
⁹⁰ Zr	1s	-52.9	33.2	-56.0	-117	33.4	-154	40.6
	1p	-40.0	30.5	-47.7	-105	32.3	-143	39.8
	2s	-21.7	26.1	-35.4	-86.4	30.7	-123	38.0
²⁰⁸ Pb	1s	-56.3	33.2	-57.5	-118	33.1	-157	40.8
	1p	-48.3	31.8	-52.6	-111	32.5	-151	40.5
	2s	-35.9	29.6	-44.9	-100	31.7	-139	39.5

Table 3. D^- , \bar{D}^0 and D^0 bound state energies (in MeV). The widths are all set to zero.

state	$D^-(1.4^2V_\omega^g)$	$D^-(V_\omega^g)$	$D^-(V_\omega^g, \text{no Coulomb})$	$\bar{D}^0(1.4^2V_\omega^g)$	$\bar{D}^0(V_\omega^g)$	$D^0(V_\omega^g)$
1s	-10.6	-35.2	-11.2	unbound	-25.4	-96.2
1p	-10.2	-32.1	-10.0	unbound	-23.1	-93.0
2s	-7.7	-30.0	-6.6	unbound	-19.7	-88.5

Our results suggest that ω , η and η' mesons should be bound in all the nuclei considered. Furthermore, the D^- meson should be bound in ²⁰⁸Pb in any case, assisted by the Coulomb force ⁷.

4. K -meson production in heavy ion collisions^{13,14}

Here our focus is the kaon production reactions, $\pi N \rightarrow \Lambda K$, in nuclear matter. We calculate the in-medium reaction amplitudes, taking into account the scalar and vector potentials for incident, final and intermediate mesons and baryons. The processes considered in the calculation, which were already established in studies for free space¹³, are shown in Fig. 3.

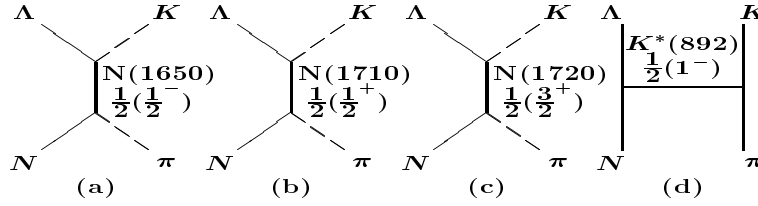


Figure 3. Processes included for the $\pi N \rightarrow \Lambda K$ reactions.

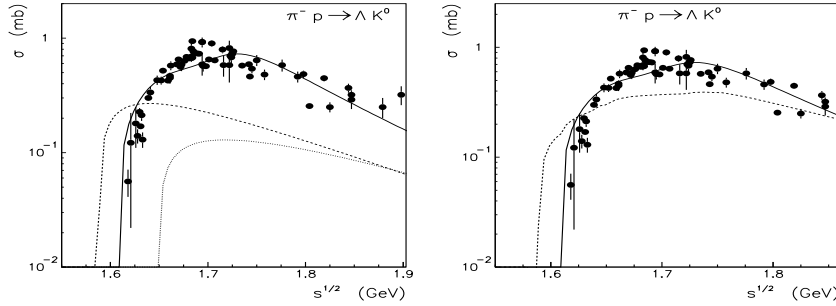


Figure 4. Energy dependence of the total cross sections. Lines in the left panel, the (solid, dashed, dotted), correspond to nuclear densities, $\rho_B = (0, \rho_0, 3\rho_0)$, respectively. Lines in the right panel, the solid and dotted, correspond to $\rho_B = 0$, and the result averaged over the nuclear density distribution in Au+Au collisions at 2A GeV¹⁴. The dots are data in free space¹⁵, $\rho_B = 0$.

Results are shown in Fig. 4. (See caption for explanations.) From the results we conclude that if one accounts for the in-medium modification of the production amplitude correctly, it is possible to understand K^+ production data in heavy ion collisions at SIS energies, even if the K^+ -meson feels the theoretically expected, repulsive mean field potential. The apparent failure to explain the K^+ production data if one includes the purely kinematic effects of the in-medium modification of the K^+ -meson and hadrons, appears to be a consequence of the omission of these effects on the reaction amplitudes.

5. J/Ψ dissociation in nuclear matter ⁸

There is a great deal of interest in possible signals of Quark-Gluon Plasma (QGP) formation, and J/Ψ suppression is a promising candidate as suggested by Matsui and Satz ¹⁶. Our interest here is how much the J/Ψ absorption cross sections in hadronic dissociation processes will be modified, if the in-medium hadron potentials are included, which has never been addressed in QGP analyses.

We consider the reactions involving the J/Ψ , shown in Fig. 5. Recent

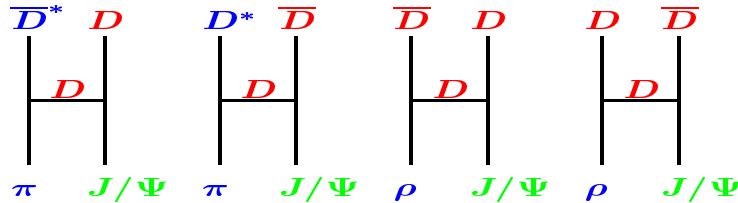


Figure 5. Processes included for J/Ψ dissociation.

calculations for the processes in free space ¹⁷, indicate a much lower cross sections than the necessary to explain the data for the J/Ψ suppression.

However, this situation changes when the in-medium potentials of the charmed (and also ρ) mesons are taken into account, as shown in the left panel of Fig. 6. Clearly, the J/Ψ absorption cross sections are substantially

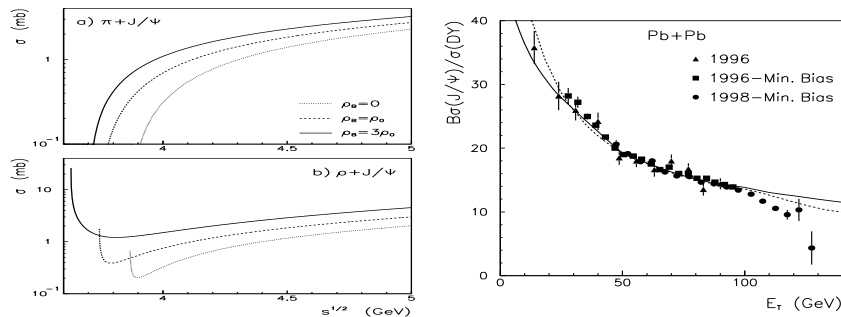


Figure 6. Energy dependence of the total cross section.

enhanced not only because of the downward shift of the reaction threshold, but also because of the in-medium effect on the reaction amplitude.

In order to compare our results with the NA38/NA50 data ¹⁸ on J/Ψ suppression in $Pb+Pb$ collisions, we have adopted the heavy ion model proposed in Ref. ¹⁹ with the E_T model from Ref. ²⁰. Our result is shown in the

right panel of Fig. 6 by the solid line, using the density dependent, thermally averaged cross section⁸. The dashed line shows the result reported in Ref.²⁰ using the phenomenological constant cross section, 4.5 mb. Both lines clearly reproduce the data¹⁸ quite well, including most recent results from NA50 on the ratio of J/Ψ over Drell-Yan cross sections, as a function of the transverse energy E_T up to about 100 GeV.

It is important to note that if one neglected the in-medium modification of the J/Ψ absorption cross section the large cross section, the large value for the J/Ψ dissociation cross section of 4.5 mb used in Ref.²⁰, could not be justified by microscopic theoretical calculations, and thus the NA50 data¹⁸ could not be described.

6. $pp \rightarrow pp\omega$ and $pp \rightarrow pp\phi$ reactions at near thresholds^{21,22}

We report here results for the vector meson production reactions at near threshold, $pp \rightarrow ppv$ ($v = \omega, \phi$)^{21,22}. Description of the model, and parameters determined by other reactions are given in Ref.²³. The vector meson production amplitude, M , is depicted in Fig. 7.

Our main results for these vector meson production are:

- (1) Tensor to vector coupling ratio, $\kappa_v \equiv f_{vNN}/g_{vNN}$, for the ω (κ_ω), where a typical NN interaction model²⁴ sets $\kappa_\omega = 0$.
- (2) ϕNN coupling constant, $g_{\phi NN}$, in connection with $s\bar{s}$ component in the nucleon wave function, and the OZI rule violation.

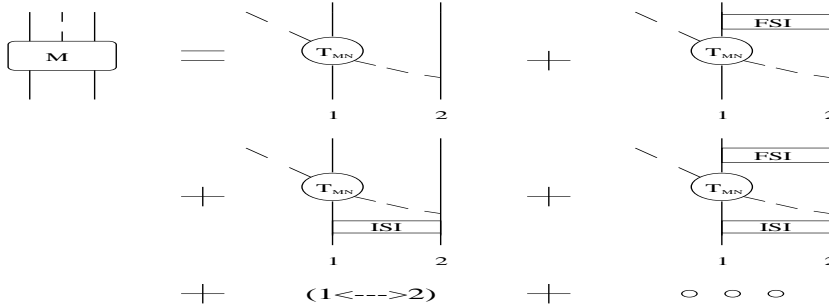


Figure 7. Amplitudes, M , for the $pp \rightarrow ppv$ ($v = \omega, \phi$) reactions considered in the study. T_{MN} , ISI and FSI stand for, meson-nucleon (MN) T-matrix, initial state interaction and final state interaction, respectively.

Results for angular distributions are shown in Fig. 8, together with the experimental data for the ω ²⁵ and ϕ ²⁶. Total contribution comes from following two sources, (1) nucleonic: the vector meson is produced from the

vNN (meson-nucleon-nucleon) vertex, and (2) mesonic: the vector meson is produced from the $v\rho\pi$ (mesonic vertex), where the π and ρ are attached to the two different protons. The ω meson production is dominated equally by the nucleonic and mesonic, while for the ϕ , the mesonic is strongly dominant. Thus, production mechanisms for these two vector mesons are different. For

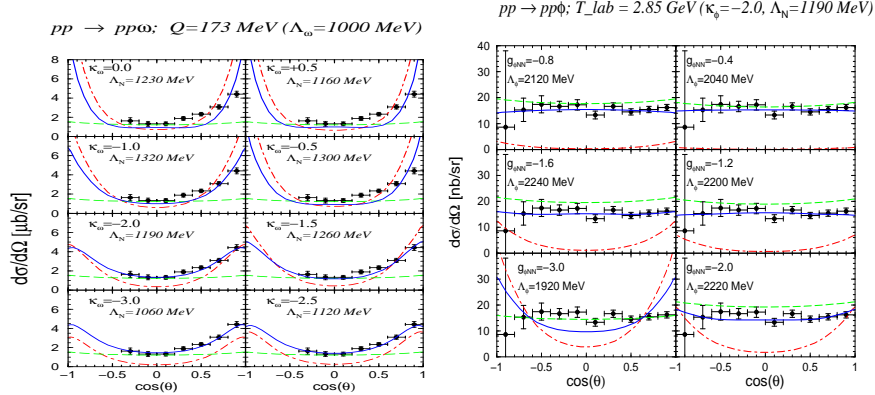


Figure 8. Angular distributions for $pp \rightarrow pp\omega$ at excess energy $Q = 173\text{MeV}$ (the left panel), and for $pp \rightarrow pp\phi$ at excess energy $Q = 83\text{MeV}$ (the right panel). They are normalized to the total cross sections, $\sigma(pp \rightarrow pp\omega) = 30.8 \mu\text{b}$ ²⁵ and $\sigma(pp \rightarrow pp\phi) = 190 \text{nb}$ ²⁶, respectively. The (solid, dash-dotted, dotted) lines correspond to the (total, nucleonic, mesonic) contributions, respectively.

the ω meson a large value $\kappa_\omega = -2.0$ with $g_{\omega NN}^2 = (-9.0)^2 = 81.0$ fits best the data²⁵, and turned out to be insensitive to the value of $g_{\omega NN}$ ^{21,22}, where in Bonn NN potential model²⁴ $\kappa_\omega = 0$ with $g_{\omega NN}^2 \simeq 24(4\pi) \simeq 301.6$ is used.

As for the ϕ meson, several parameter sets can possibly reproduce the data²⁶. Surprisingly, for $\kappa_\phi = -2.0$, a large absolute value $|g_{\phi NN}| = |-2.0|$, can also reproduce the data. This implies a large violation of the OZI rule. However, this turned out to give a distinguishable, different energy dependence for the total cross section at near threshold²². Thus, we can distinguish if energy dependence of the total cross section is measured at near threshold.

7. Conclusion

In conclusion, there are many motivations and rich phenomena for performing experiments to study the changes in hadron properties in nuclear medium, or to study the partial restoration of chiral symmetry in nuclear medium.

Acknowledgments

The author would like to thank, D.H. Lu, K. Nakayama, K. Saito, A. Sibirtsev and A.W. Thomas for exciting collaborations, and a warm hospitality at CSSM during the workshop. Special thanks go to Prof. A.W. Thomas for many

supports to attend the workshop possible. This work was partially supported by the Forschungszentrum-Jülich, contract No. 41445282 (COSY-058).

References

1. P.A.M. Guichon, *Phys. Lett.* **B200** (1989) 235.
2. P.A.M. Guichon et al., *Nucl. Phys.* **A601** (1996) 349; K. Saito, K. Tsushima, A.W. Thomas, *Phys. Rev.* **C55**, 2637 (1997); *Phys. Rev.* **C56**, 566 (1997); D.H. Lu et al., *Nucl. Phys.* **A634**, 443 (1998); G. Krein, A.W. Thomas, K. Tsushima, *Nucl. Phys.* **A650**, 313 (1999).
3. K. Saito, K. Tsushima, A.W. Thomas, *Nucl. Phys.* **A609** (1996) 339.
4. K. Tsushima, K. Saito, A.W. Thomas, *Phys. Lett.* **B411**, 9 (1997); (E) *ibid* **B421**, 413 (1998); K. Tsushima et al., *Nucl. Phys.* **A630** (1998) 691.
5. K. Tsushima et al., *Phys. Lett.* **B429** (1998) 239; (E) *ibid* **B436** (1998) 453.
6. K. Tsushima et al., *Phys. Lett.* **B443** (1998) 26; K. Tsushima, in the proceeding, *ISHEP 98*, Dubna, Russia, 17-22 Aug 1998, nucl-th/9811063; *Nucl. Phys.* **A670**, 198c (2000); K. Tsushima et al., *Nucl. Phys.* **A680**, 280c (2001).
7. K. Tsushima et al., *Phys. Rev.* **C59** (1999) 2824.
8. A. Sibirtsev et al., *Phys. Lett.* **B484**, 23 (2000).
9. A. Sibirtsev, K. Tsushima, A.W. Thomas, *Eur. Phys. J.* **A6**, 351 (1999).
10. J.D. Walecka, *Ann. Phys. (NY)* **83**, 491 (1974); B.D. Serot and J.D. Walecka, *Adv. Nucl. Phys.* **16**, 1 (1986).
11. R.E. Chrien, *Nucl. Phys.* **A478**, 705c-712c (1988).
12. K. Saito et al., *Phys. Rev.* **C59** (1999) 1203.
13. K. Tsushima, S.W. Huang, A. Faessler, *Phys. Lett.* **B337**, 245 (1994); *J. Phys.* **G21**, 33 (1995); *Aust. J. Phys.* **50**, 35 (1997); K. Tsushima et al., *Phys. Rev.* **C59**, 369 (1999); *ibid*, (E) **C61**, 029903 (2000).
14. K. Tsushima, A. Sibirtsev, A.W. Thomas, *Phys. Rev.* **C62**, 064904 (2000); *J. Phys.* **G27**, 349 (2001).
15. Landolt-Börnstein, *New Series*, ed. H. Schopper, **8** (1973).
16. T. Matsui and H. Satz, *Phys. Lett.* **B178**, 416 (1986).
17. S.G. Matinyan and B. Müller, *Phys. Rev.* **C58**, 2994 (1998); B. Müller, *Nucl. Phys.* **A661**, 272 (1999).
18. Quark Matter '97, *Nucl. Phys.* **A638** (1998); M. C. Abreu et al. (NA50 Collaboration), *Phys. Lett.* **B410**, 337 (1997); *Phys. Lett.* **B450**, 456 (1999); M. C. Abreu et al. (NA50 Collaboration), *Phys. Lett.* **B477**, 28 (2000).
19. N. Armesto and A. Capella, *J. Phys.* **G23** 1969, (1997); *Phys. Lett.* **B430**, 23 (1998); N. Armesto, A. Capella and E.G. Ferreira, *Phys. Rev.* **C59**, 395 (1999).
20. A. Capella, E.G. Ferreira and A.B. Kaidalov, *Phys. Rev. Lett.* **85**, 2080 (2000).
21. K. Nakayama, K. Tsushima, in preparation.
22. K. Tsushima, K. Nakayama, in preparation.
23. K. Nakayama et al., *Phys. Rev.* **C57**, 1580 (1988); *Phys. Rev.* **C60**, 055209 (1999); *Phys. Rev.* **C61**, 024001 (1999); K. Nakayama, J. Speth, T.-S.H. Lee, *Phys. Rev.* **C65**, 045210 (2002).
24. R. Machleidt, *Adv. Nucl. Phys.* **19**, 189 (1989).
25. S. Abd El-Samad et al. (COSY-TOF collaboration), *Phys. Lett.* **B522**, 16 (2001).
26. F. Balestra et al. (DISTO collaboration), *Phys. Rev.* **C63**, 024004 (2001).